Int. J. Adv. Appl. Math. and Mech. 8(2) (2020) 1 – 14 (ISSN: 2347-2529)

Journal homepage: www.ijaamm.com

IJAAMM

International Journal of Advances in Applied Mathematics and Mechanics

Dusty Fluid Flow Past between Two Parallel Riga Plates Embedded in a Porous Medium

Research Article

M. R. Islam[a,*], S. Nasrin[b]

[a]*Department of Mathematics, Bangabandhu Sheikh Mujibur Rahman Science and Technology University, Gopalganj-8100, Bangladesh*

[b]*Department of Mathematics, Jagannath University, Dhaka-1100, Bangladesh*

Received 06 July 2020; accepted (in revised version) 19 October 2020

Abstract: The present study is carried out on the unsteady laminar heat transferable dusty fluid flow past between two parallel Riga plates. Both the plates have been chosen stationary. The fluid is kept in motion by applying a uniform magnetic force which is influenced by the Riga plate and by a pressure gradient force on the fluid. The governing equations are derived from Navier-Stokes equation, Energy equation and boundary layer approximation has been employed. The motion of the dust particles including stresses is governed by Newton's second law. The non-dimensional equations are solved by using an explicit finite difference method. The effects of relevant parameters on the velocity and temperature distributions as well as the shear stress and Nusselt number of clean fluid particle and dust particles have been discussed in detail and shown graphically.

MSC: 76W05 • 65M06

Keywords: MHD Fluid • Dust Particle • Riga Plate • Porous Medium • Explicit Finite Difference

1. Introduction

Studies connected to flow and heat transfer of dusty fluids along parallel plates are highly effective in the fields of environmental pollution, fluidization, combustion, petroleum, polymer and geophysical procedures, refrigeration, polluted soil, air and water, dust or fumes in the gas cooling system, in agriculture, crude oil purifying, polymer technology and dye systems. Riga plate is the combination of electrodes and permanent magnets that create a plane surface instead of polarity and magnetization. This order produces the electromagnetic hydrodynamic fluid behavior and minimizes the friction and pressure drug. Gailitis and Leilausis(1961) are pioneers of the Riga plate where the plate generates a wall paralleled Lorentz force to control the fluid flow. When the most important feature of the Greenberg-term appears, many writers are interested in working on the Riga plate. Pantokratoras and Magyari [2] proposed an electromagnetic actuator or Riga plate of an electro-magneto hydrodynamic free convection flow of a conducting fluid. Wahidunnisa et al. [3] studied on the heat source of nanofluid flow through a Riga plate with viscous dissipation. Anjum et al. [4] explained the thermally stratified viscous fluid with stagnation point flow dominated by a variable thicked non-linear Riga plate. Ahmad [5] studied the effect of the Powell - Eyring and Reiner-Phillipoff fluid flow on the Riga plate. The characteristics of nano fluid boundary layer flow occupied with a Riga plate is concerned by Hayat et al. [6]. Iqbal et al. [7] and [8] investigated an electrically conducting Riga-plate on viscous nanofluid with the reach of viscous dissipation and thermal radiation and melting heat. They proposed the erratic thickness of the

* Corresponding author.

E-mail address(es): mribsmrstu@yahoo.com (M. R. Islam).

Nomenclature:
('∧' on variable means dimensional quantities)

$\hat{u}$	clean fluid velocity component along $\hat{x}$ -axis
$\hat{v}$	clean fluid velocity component along $\hat{y}$ - axis
$\hat{w}$	clean fluid velocity component along $\hat{z}$ - axis
$\hat{u}_p$	dust particle velocity component along $\hat{x}$ -axis
$\hat{v}_p$	dust particle velocity component along $\hat{y}$ -axis
$\hat{w}_p$	dust particle velocity component along $\hat{z}$ -axis
$\hat{p}$	pressure on the fluid
$\hat{t}$	time
υ	kinematic viscosity of the clean fluid
κ	permeability of the porous medium
m_p	average mass of the of dust particle
ρ	density of clean fluid
ρ_p	material density of dust particle
c_s	specific heat capacity
k	thermal conductivity of the fluid
c_p	specific heat at constant pressure
h	height
$\hat{\mathbf{J}}$	current density
$\hat{\mathbf{B}}$	induced magnetic field vector
a	average radius of the of dust particle
$\hat{T}$	temperature of the fluid
$\hat{T}_p$	temperature of the dust particle
$\hat{T}_1$	temperature of the lower plate
$\hat{T}_2$	temperature of the lower plate
u	clean fluid velocity component along x -axis
u_p	dust particle velocity component along x -axis
α	pressure gradient
θ	temperature of the clean fluid
θ_p	temperature of the dust particle
β	stresses coefficient
H_r	modified Hartmann number
R	fluid concentration parameter
G	particle mass parameter
P_r	Prandtl number
E_c	Eckert number
L_0	Relaxation time parameter.
t	time
Δt	time increment
K	Stokes constant = $6\pi\rho\upsilon a$
N	number of dust particles per unit volume
γ_T	temperature relaxation time
τ_L	local shear stress of clean fluid
τ_{pL}	local shear stress of dust particle
τ_A	average shear stress of clean fluid
τ_{pA}	average shear stress dust particle
Nu_L	local Nusselt number of clean fluid
Nu_{pL}	local Nusselt number of dust particle
Nu_A	average Nusselt number of clean fluid
Nu_{pA}	average Nusselt number of dust particle

stagnation point flow over the Riga plate. Ayub et al. [9] examined the effect of EMHD nanofuid flow along a Riga plate. Ahmed et al. [10] are conferred on the mixed convection boundary layer flow along a vertical Riga plate in the presence of strong suction of a nanofluid. Ghulam Rasool et al. [11-12] investigated the effect of a chemical reaction on the Marangoni flow of the convective flow of nanofluids in the presence of Lorentz force and thermal radiation. Also, they have studied on the second grade of nanofluidic flow past a provocative heated vertical Riga plate.

Dusty fluid flows have a special two-phase nature that the fluid mixed with dust. When raindrops have been fallen then the combination of small dust particles in the air with water, extraction of oil and gas from the ground are the perfect examples of dusty fluids. Last few years (2014-2019) many authors have been analyzed the phenomenon of dust particles of Newtonian and non-Newtonian fluids with or without heat transfer between parallel plates [13–17].

Eguia et al. [18] achieved an accurate prediction of the flow and heat transfer of dusty fluid flow between parallel plates influence of a magnetic field. Hazarika and Hazarika [19] investigated the dusty fluid flow along a moving plate with thermal conductivity and variable viscosity. Dusty fluid flow along a channel with a magnetic field also has significant applications in engineering, chemical industry, purification air and oil, wear systems, pumps and generators [20–22]. The authors [23–25] studied on the dusty fluid with heat transfer on the stretching surface for a wide range of uses in engineering, industrial and chemical processing, in air conditioning, refrigeration and nuclear reactors. Yabo et al. [26] considered the unsteady free convection Couette flow with the effect of the transverse magnetic field and the thermal radiation. Ismail et al. [27] examined the MHD dusty fluid flow between parallel porous plate with the effect of a transverse magnetic field. Srivastava and Khare [28] prescribed the effect of heat and mass transfer of an electrically conducting incompressible fluid between two parallel plates in the presence of a magnetic field.

From the above discussion, it concludes that no author has given any idea about the Riga plate with dusty fluid. Our aim is the flow of dusty fluid between two parallel Riga plates set in a porous medium is investigated numerically and the behavior of the flow properties is discussed and presented graphically.

2. Problem formulation

Let us consider an unsteady incompressible laminar flow of viscous dusty fluid between two horizontal parallel Riga plates embedded in a porous medium. Let both the plates is kept stationary, the lower plate is rest at $\hat{y} = -h$ while the upper plate at $\hat{y} = h$. The direction of the flow be taken along the $x-$ axis, the $\hat{y}-$ axis is perpendicular to the flow and width of the plates parallel to the $\hat{x}\hat{z}-$ plane. The fluid is kept in motion by applying a pressure gradient force $\frac{\partial \hat{p}}{\partial \hat{x}}$, also a uniform magnetic force is applied on the fluid, which is influenced by the Riga plate. The velocity components $\hat{v}$ and $\hat{w}$ are zero everywhere at the plate. For dust particle, $\hat{v}_p$ and $\hat{w}_p$ are also zero everywhere. Consider the plate is long enough in $x-$ direction and the fluid motion is two dimensional. But the continuity equation reduces to for the fluid phase $\frac{\partial \hat{u}}{\partial \hat{x}} = 0 \Rightarrow \ \hat{u} = \hat{u}(\hat{y}, \hat{t})$ and for dust phase $\frac{\partial \hat{u}_p}{\partial \hat{x}} = 0 \Rightarrow \ \hat{u}_p = \hat{u}_p(\hat{y}, \hat{t})$. The two plates are fixed at two constant temperatures; $\hat{T}_1$ for the lower and $\hat{T}_2$ for the upper plate, where $\hat{T}_2 > \hat{T}_1$. The physical model is shown in Fig.1.

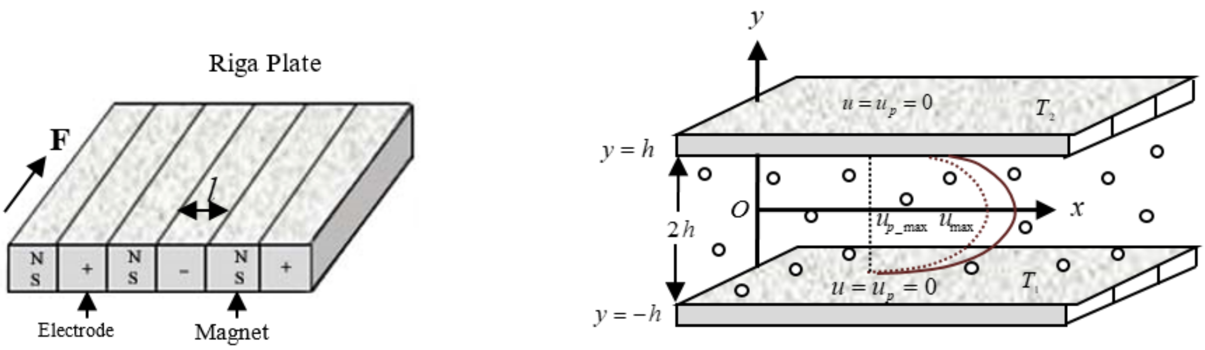

Fig. 1.

Due the Riga plate, the Lorentz force $\bar{f} = \hat{\mathbf{J}} \wedge \hat{\mathbf{B}} \approx \sigma(\hat{\mathbf{E}} \wedge \hat{\mathbf{B}})$ is defined as magnetic force. According to the Grinberg hypothesis this magnetic forces is defined as follows: $\bar{f} = \hat{\mathbf{J}} \wedge \hat{\mathbf{B}} = \left(\frac{\pi}{8} J_0 M_0 e^{-\frac{\pi}{l}\hat{y}} \text{ , } 0 \text{ , } \frac{\pi}{8} J_0 M_0 e^{-\frac{\pi}{l}\hat{y}} \right)$

Under the consideration of above assumptions, and also applying Boussinesq approximation on the fluid, the dimensional forms of the momentum and energy equations for the clean fluid and the dust particle are reduced to the equations as follows:

$$\frac{\partial \hat{u}}{\partial \hat{t}} = -\frac{1}{\rho}\frac{\partial \hat{p}}{\partial \hat{x}} + \upsilon \frac{\partial^2 \hat{u}}{\partial \hat{y}^2} + \frac{\pi}{8\rho} J_0 M_0 e^{-\frac{\pi}{l}\hat{y}} - \frac{1}{\rho} KN(\hat{u} - \hat{u}_p) - \frac{\upsilon}{\kappa}\hat{u} \tag{1}$$

$$m_p \frac{\partial \hat{u}_p}{\partial \hat{t}} = KN(\hat{u} - \hat{u}_p) \tag{2}$$

$$\frac{\partial \hat{T}}{\partial \hat{t}} = \frac{k}{\rho c_p}\frac{\partial^2 \hat{T}}{\partial \hat{y}^2} - \frac{\rho_p c_s}{\rho c_p \gamma_T}\left(\hat{T} - \hat{T}_p\right) + \frac{\upsilon}{c_p}\left(\frac{\partial \hat{u}}{\partial \hat{y}}\right)^2 \tag{3}$$

$$\frac{\partial \hat{T}_p}{\partial \hat{t}} = \frac{1}{\gamma_T}(\hat{T} - \hat{T}_p) \tag{4}$$

The corresponding boundary conditions are

$$\left.\begin{array}{l} \hat{u}=0,\ \hat{u}_p=0,\ \hat{T}=\hat{T}_1,\ \hat{T}_p=\hat{T}_1 \text{ at } \hat{y}=-h \\ \hat{u}=0,\ \hat{u}_p=0,\ \hat{T}=\hat{T}_2,\ \hat{T}_p=\hat{T}_2 \text{ at } \hat{y}=h \end{array}\right\} \tag{5}$$

where, $\hat{u}, \hat{v}, \hat{w}$ are the clean fluid velocity components, $\hat{u}_p, \hat{v}_p, \hat{w}_p$ are the dust particles velocity components, v is the kinematic viscosity of the clean fluid, κ is the permeability of the porous medium, $\hat{\mathbf{J}} = (J_x, J_y, J_z)$ is the current density, $\hat{\mathbf{B}} = (B_x, B_y, B_z)$ is the induced magnetic field vector, N is the number of dust particles per unit volume, K is the Stokes constant $= 6\pi\rho v a$; a is the average radius of the of dust particles, m_p is the average mass of the of dust particles, ρ_p is the material density (or mass per unit volume) of dust particles, c_s is the is the specific heat capacity of the particles, T is the temperature of the fluid, T_p is the temperature of the dust particles, k is thermal conductivity of the fluid, c_p is the specific heat capacity at constant pressure, γ_T is the temperature relaxation time which may defined by $\gamma_T = \frac{\rho_p c_s}{4k\pi a N}$ or $\frac{3\rho v \rho_p c_s}{2kKN}$ as the energy equation (3) leads to the equation:

$$\frac{\partial \hat{T}}{\partial \hat{t}} = \frac{k}{\rho c_p}\frac{\partial^2 \hat{T}}{\partial \hat{y}^2} - \frac{2kKN}{3\rho^2 c_p v}\left(\hat{T} - \hat{T}_p\right) + \frac{v}{c_p}\left(\frac{\partial \hat{u}}{\partial \hat{y}}\right)^2 \tag{6}$$

The dust particles motion including stresses, Newton's second law (2) gives the following form:

$$m_p\frac{\partial \hat{u}_p}{\partial \hat{t}} = \mu_p\frac{\partial^2 \hat{u}_p}{\partial \hat{y}^2} + KN(\hat{u} - \hat{u}_p) \tag{7}$$

Now introducing the non-dimensional variables are as follows:

$$x = \frac{\pi}{l}\hat{x}, \quad y = \frac{\pi}{l}\hat{y}, \quad u = \frac{l}{\pi v}\hat{u}, \quad u_p = \frac{l}{\pi v}\hat{u}_p,$$
$$p = \frac{l^2\tilde{p}}{\pi^2\rho v^2}, \quad t = \frac{\pi^2 v}{l^2}\hat{t}, \quad \theta = \frac{\hat{T}-\hat{T}_1}{\hat{T}_2-\hat{T}_1}, \quad \theta_p = \frac{\hat{T}_p-\hat{T}_1}{\hat{T}_2-\hat{T}_1},$$

Applying these into the above equations, yields

$$\frac{\partial u}{\partial t} = \alpha + \frac{\partial^2 u}{\partial y^2} + H_r\, e^{-y} - R\,(u - u_p) - \frac{u}{K} \tag{8}$$

$$\frac{\partial u_p}{\partial t} = \beta\frac{\partial^2 u_p}{\partial y^2} + \frac{1}{G}\left(u - u_p\right) \tag{9}$$

$$\frac{\partial \theta}{\partial t} = \frac{1}{P_r}\frac{\partial^2 \theta}{\partial y^2} - \frac{2R}{3P_r}\left(\theta - \theta_p\right) + E_c\left(\frac{\partial u}{\partial y}\right)^2 \tag{10}$$

$$\frac{\partial \theta_p}{\partial t} = L_0\left(\theta - \theta_p\right) \tag{11}$$

The corresponding boundary conditions are

$$\left.\begin{array}{l} u=0,\ u_p=0,\ \theta=0,\ \theta_p=0 \text{ at } y=-h \\ u=0,\ u_p=0,\ \theta=1,\ \theta_p=1 \text{ at } y=h \end{array}\right\} \tag{12}$$

where,

$\alpha = -\frac{\partial p}{\partial x}$ is the dimensionless pressure gradient;

$\beta = \frac{\mu_p}{m_p v}$ = Dimensionless stresses coefficient per unit volume;

$H_r = \frac{l^3 J_0 M_0}{8\rho v^2 \pi^2}$ = Modified Hartmann Number;

$R = \frac{KNl^2}{\rho v \pi^2}$ = Fluid concentration parameter;

$G = \frac{m_p v \pi^2}{Kl^2}$ = Particle mass parameter;

$P_r = \frac{\rho c_p v}{k}$ = Prandtl number;

$E_c = \frac{v^2\pi^2}{c_p l^2(\tilde{T}_2 - \tilde{T}_1)}$ = Eckert number

$L_0 = \frac{l^2}{v\pi^2\gamma_T}$ = Temperature relaxation time parameter.

3. Method of solution

The explicit finite difference method has been applied to solve the non-dimensional coupled partial differential equations (8)-(11) together with associated boundary conditions (12). It is considered maximum length of the plate is $x_{\max}(=15)$ and distance between the plates $h=2$ i.e. $y_{\max}=1$ as the lower plate is fixed at $y_{\min}=-1$. This means x varies from 0 to 15 and y varies from -1 to 1 . The finite difference schemes for the problems are as follows:

$$\frac{U_{i,j}^{k+1}-U_{i,j}^{k}}{\Delta t}=\alpha+\frac{U_{i,j+1}^{k}-2U_{i,j}^{k}+U_{i,j-1}^{k}}{\Delta y^2}+H_r\,e^{-y_i}-R\,(U_{i,j}^{k}-Up_{i,j}^{k})-\frac{U_{i,j}^{k}}{K}$$

$$\frac{Up_{i,j}^{k+1}-Up_{i,j}^{k}}{\Delta t}=\beta\left(\frac{Up_{i,j+1}^{k}-2Up_{i,j}^{k}+Up_{i,j-1}^{k}}{\Delta y^2}\right)+\frac{1}{G}\left(U_{i,j}^{k}-Up_{i,j}^{k}\right)$$

$$\frac{\Theta_{i,j}^{k+1}-\Theta_{i,j}^{k}}{\Delta t}=\frac{1}{P_r}\left(\frac{\Theta_{i,j+1}^{k}-2\Theta_{i,j}^{k}+\Theta_{i,j-1}^{k}}{\Delta y^2}\right)-\frac{2R}{3P_r}\left(\Theta_{i,j}^{k}-\Theta p_{i,j}^{k}\right)+E_c\left(\frac{U_{i,j}^{k}-U_{i,j-1}^{k}}{\Delta y}\right)^2$$

$$\frac{\Theta p_{i,j}^{k+1}-\Theta p_{i,j}^{k}}{\Delta t}=L_0\left(\Theta_{i,j}^{k}-\Theta p_{i,j}^{k}\right)$$

with boundary conditions

$$U_{i,L}=0,\ \ Up_{i,L}=0,\ \ \Theta_{i,L}=0,\ \ \Theta p_{i,L}=0 \text{ at } L=-1$$
$$U_{i,L}=0,\ \ Up_{i,L}=0,\ \ \Theta_{i,L}=1,\ \ \Theta p_{i,L}=1 \text{ at } L=1$$

Shear stresses, Nusselt number and Sherwood number: The effects of pertinent parameters on the local and average shear stress from the velocity of fluid phase and dust particle phase have investigated. The non-dimensional form of the local and average shear stress for the fluid phase are given by the relations $\tau_L=\mu\frac{\partial u}{\partial y}\Big|_{y=0}$ and $\tau_A=\frac{1}{L}\int_0^L\mu\frac{\partial u}{\partial y}\Big|_{y=0}dx$ and for the dust particle are given by $\tau_{pL}=\mu\frac{\partial u_p}{\partial y}\Big|_{y=0}$ and $\tau_{pA}=\frac{1}{L}\int_0^L\mu\frac{\partial u_p}{\partial y}\Big|_{y=0}dx$ respectively. The rate of heat transfer at the plate is defined as the Nusselt number. The local and average Nusselt number for the fluid phase are given by $Nu_L=-\mu\frac{\partial\theta}{\partial y}\Big|_{y=0}$ and $Nu_A=-\frac{1}{L}\int_0^L\mu\frac{\partial\theta}{\partial y}\Big|_{y=0}dx$ and for the dust particle are given by $Nu_{pL}=-\mu\frac{\partial\theta_p}{\partial y}\Big|_{y=0}$ and $Nu_{pA}=-\frac{1}{L}\int_0^L\mu\frac{\partial\theta_p}{\partial y}\Big|_{y=0}dx$ respectively.

4. Results and Discussions

relevant non-dimensional parameters namely pressure gradient parameter (α) , the dimensionless stresses parameter (β) , modified Hartmann number (H_r) , fluid concentration parameter (R), particle mass parameter (G) , Eckert number (E_c) , Prandtl number (P_r) and temperature relaxation time parameter (L_0) on the non-dimensional velocity u (oru_p) and temperature θ (orθ_p) . The effects of those parameters on some necessary profiles are investigated with the fixed values of $\alpha=1$, $\beta=1$, $K=1.0$, $H_r=1.0$, $R=0.5$, $G=0.5$, $E_c=0.01$, $P_r=7.0$, $L_0=0.8$.

Steady-state solution: To get steady-state solutions, distributions need to be shown for different periods of time. The fluid velocity distribution u and dust particle temperature θ_p have described for different time τ , which are illustrated in Fig.2(a) and Fig.2(b). The computations have been found for the different time such as $\tau=1,2,3,4,5,6$ for u and time $\tau=8,12,16,18,19,20$ for θ_p with the time step $\Delta t=0.0005$. There is negligible change between time $\tau=2$ and $\tau=3$ for u and between $\tau=18$ and $\tau=20$ for θ_p . Fig.2 (c) depicts the validity of the grid pairs on the temperature θ . The velocity distribution for three grid pairs $(m,n)=(40,40)$, $(m,n)=(50,50)$ and $(m,n)=(60,60)$ with time $\tau=20$ and time step $\Delta t=0.0005$. There is also negligible change among these grid pairs so that anyone grid pair is acceptable to find the steady-state solution. It has seen the same situation for the other distributions. The steady-state solution has performed at least $\tau>2$ for velocity and at least $\tau>20$ for temperature. In the present analysis, the following graphs have established for the choice of time $\tau=20$ with the grid pair $(m,n)=(50,50)$ and time step $\Delta t=0.0005$.

Effects of various parameters: It is mentioned that in each figure of Figs.3-12, the solid line plot has indicated the distribution for the fluid phase and the dotted line plot has indicated the distribution for the dust particle phase. The effects of the dimensionless pressure gradient α on the velocity for fluid and dust particles, which are shown in Figs.3(a)-(c). The velocity u (oru_p) has increasing effect with the increase of α over the entire width between the plates. The same situation occurred for the local and average shear stress on the clean fluid and dust particles, which

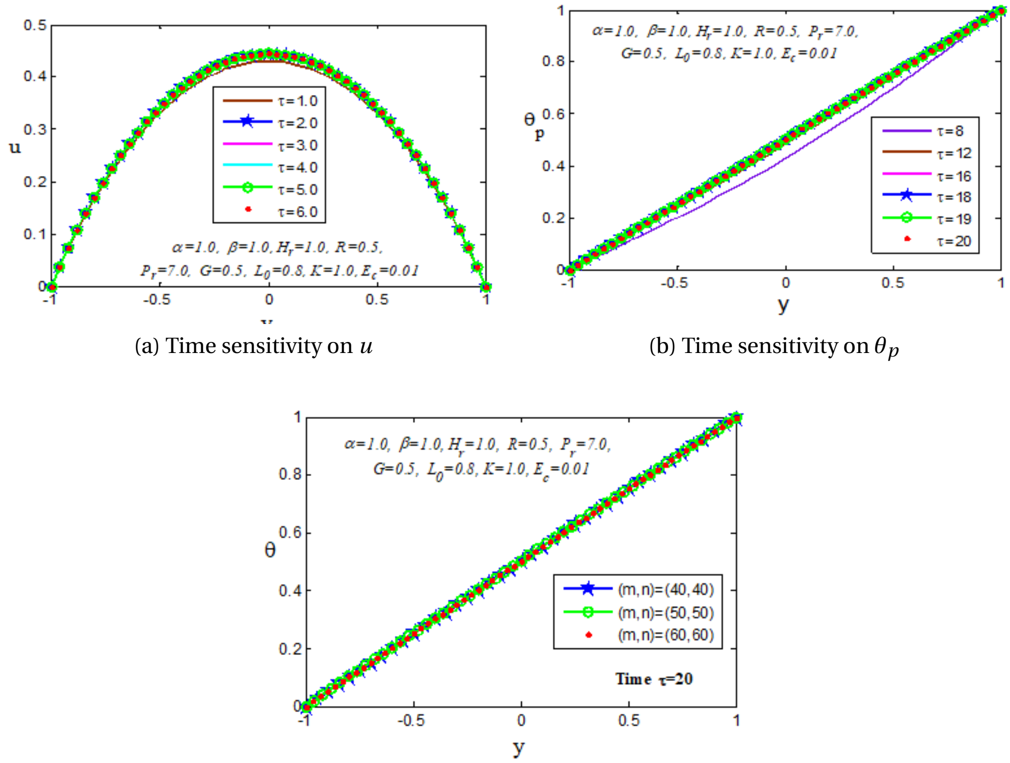

(a) Time sensitivity on u

(b) Time sensitivity on θ_p

(c) Mesh sensitivity on θ

Fig. 2.

have shown in Figs.3 (b) and (c) respectively. It has shown from figures that the velocities of the clean fluid particles faster than dust particles and the maximum velocities have occurred in the central line direction.

Figs.4(a)-(c) illustrate the effects of dimensionless stress parameter β on velocity u (oru_p) , local shear stress τ_L (orτ_{pL}) and on the average shear stress τ_A (orτ_{pA}) respectively. Fig.4(a) shows that both the velocities have decreasing effect with the increase of β over the entire width between the plates. On the other hand the local (and average) shear stress on the clean fluid and dust particle both have decreasing effect with the increase of β which have shown in Figs.4(b) and (c) respectively

Figs.5(a)-(c) depict the variations on the velocity u (oru_p) , local shear stress τ_L (orτ_{pL}) and on the average shear stress τ_A (orτ_{pA}) with the effect of modified Hartmann number H_r respectively. It has shown that u, τ_L and τ_A are all increased with the increase of H_r . Also u_p, τ_{pL} and τ_{pA} of the dust particle are increased with the increase of H_r .

Figs.6(a)-(c) influence the effects of fluid concentration parameter R on the velocity u (oru_p) , local shear stress τ_L (orτ_{pL}) and on the average shear stress τ_A (orτ_{pA}) respectively. It has displayed that u, τ_L and τ_A decreases with the increase of R . The dust particle has also shown the same behavior. But dust particle velocity slower than clean fluid particle.

Figs.7(a)-(c) indicate the variations with particle mass parameter G on the velocity u (oru_p) , local shear stress τ_L (orτ_{pL}) and on the average shear stress τ_A (orτ_{pA}) respectively. It has seen that u, τ_L and τ_A are all decreased with the increase of G . For the dust particle, they have shown the same results. Here is also the dust particle velocity slower than clean fluid particle.

The variations of the porous parameter K on the velocity u (oru_p) , local shear stress τ_L (orτ_{pL}) and on the average shear stress τ_A (orτ_{pA}) are presented in Figs.8(a)-(c). Higher values of G displayed the higher velocities u, local shear stress τ_L and average shear stress τ_A . Dust particle has given that the same results.

Figs.9-12 present the influence of the temperature distribution, shear stress and Nusselt number for the different values of E_c , G , L_0 and P_r . Fig.9(a) shows that temperature increases with increase of E_c for both fluid and dust particle. Local and average Nusselt number has decreasing effect with increase of E_c , which are shown in Fig.9(b) and Fig.9(c) respectively.

The effect of G on θ (orθ_p) has shown in Fig.10(a). The temperature θ (orθ_p) decreases but it has very minor effect on P_r . It's clear effects has shown in the zoom box keep in Fig.10(a). As well as its corresponding local and average Nusselt number has increasing effect, which are displayed in Fig.10(b) and Fig.10(c).

Fig.11(a) and Fig.12(a) depicts that increase in L_0 and P_r the temperature θ (orθ_p) has very minor increasing behavior. The attached zoom figures have shown its clear variations. Its corresponding local Nusselt number Nu_L (orNu_{pL})

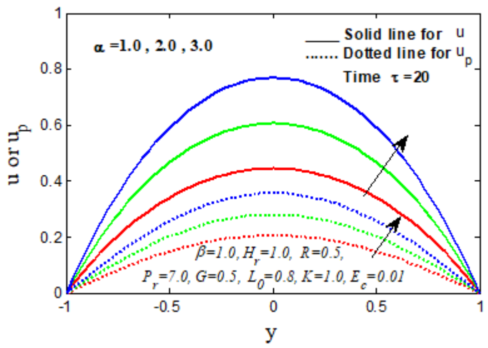

(a) Effect of α on u (oru_p)

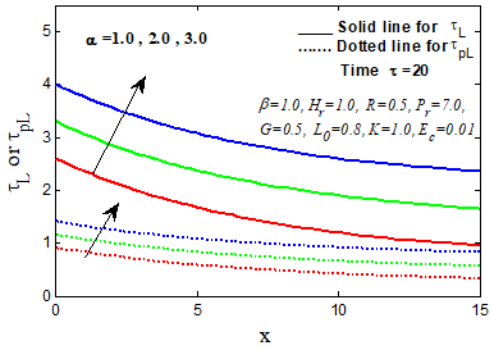

(b) Effect of α on τ_L (orτ_{pL})

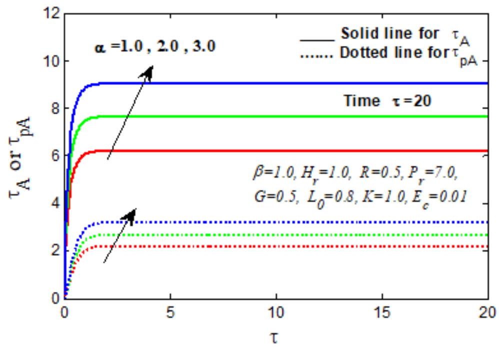

(c) Effect of α on τ_A (orτ_{pA})

Fig. 3.

is illustrated in Fig.11(b) and Fig.12(b). It is observed from both figures that local Nusselt number decreases with the increase of L_0 and P_r respectively.

Also the average Nusselt number Nu_A (orNu_{pA}) decreases with L_0 , while it increases with a fixed number of time step thereafter it has decreasing effect until steady-state solution with the increase of P_r , which are illustrated in Fig.11(c), Fig.12(c).

5. Conclusions

It is concluded that the fluid particle is faster than the dust particle and they are likely parallel to each other. To reaches a steady-state solution the velocity is faster than the temperature. The velocity of the dust particle does not coincide with a fluid particle at a steady-state situation but the temperature of them is in equilibrium after a certain time step. Others some important findings are described as follows:

- The velocities u and u_p are risen with the increase of α , H_r and K , while it has decreasing effects with the increase of β , R and G .
- The temperature θ and θ_p increases with increase of E_c , L_0 and P_r , while it has decreasing effect with G .
- The same effects of velocities have found for the local and average shear stress of both fluid and dust particle.
- But for the temperature the thermal boundary layer thickness as well as heat transfer rate at the plate have shown the reverse effects of temperature distribution for both fluid and dust particle.

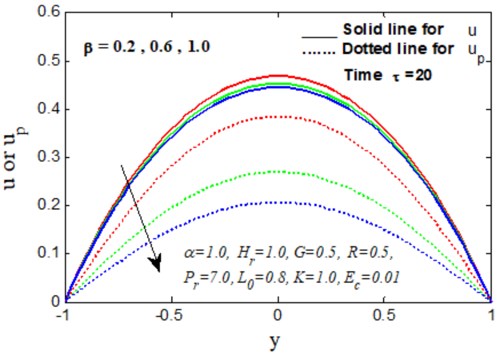

(a) Effect of β on u (oru_p)

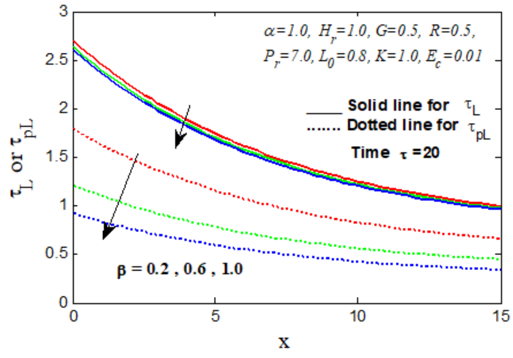

(b) Effect of β on τ_L (orτ_{pL})

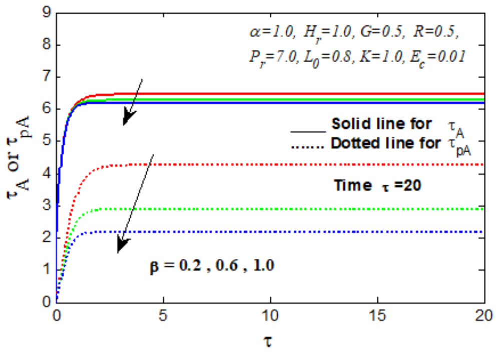

(c) Effect of β on τ_A (orτ_{pA})

Fig. 4.

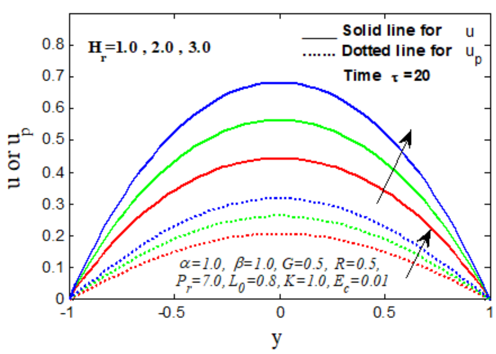

(a) Effect of H_r on u (oru_p)

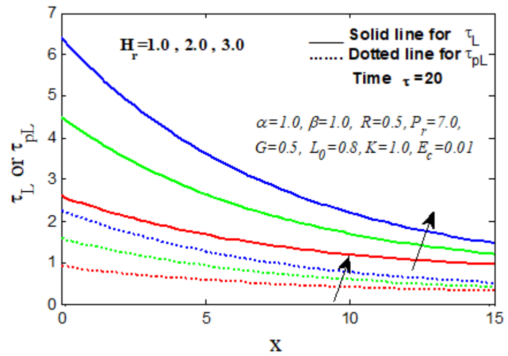

(b) Effect of H_r on τ_L (orτ_{pL})

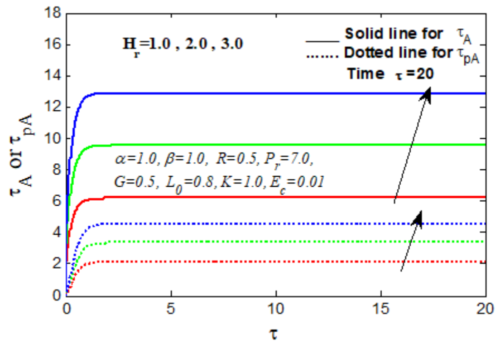

(c) Effect of H_r on τ_A (orτ_{pA})

Fig. 5.

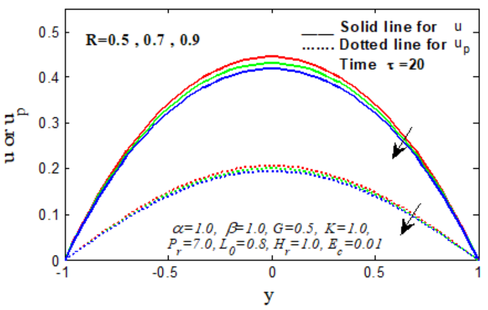

(a) Effect of R on u (oru_p)

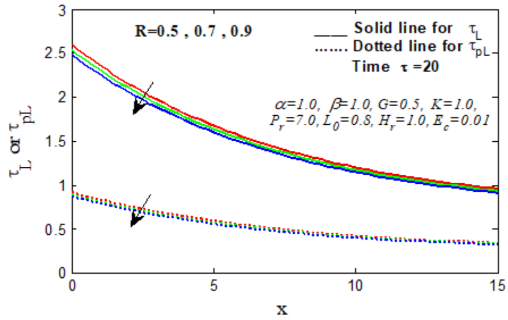

(b) Effect of R on τ_L (orτ_{pL})

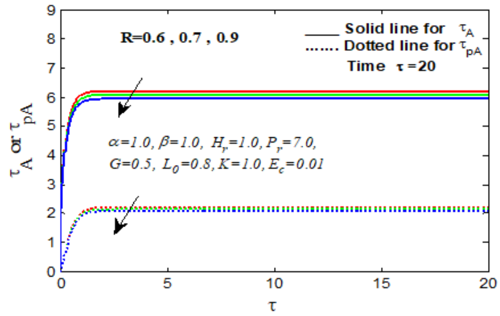

(c) Effect of R on τ_A (orτ_{pA})

Fig. 6.

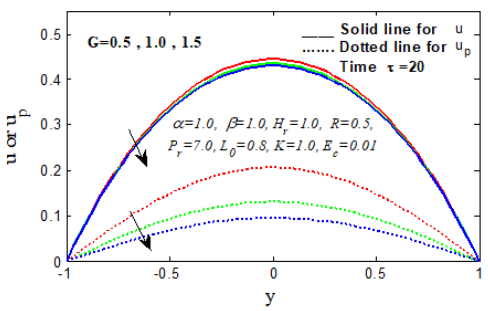

(a) Effect of G on u (oru_p)

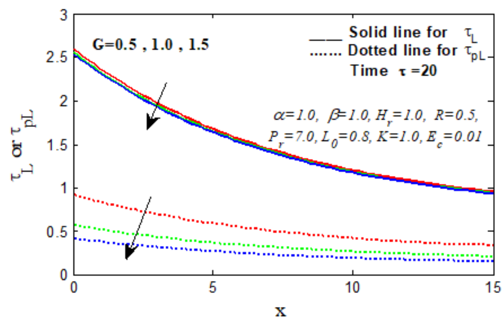

(b) Effect of G on τ_L (orτ_{pL})

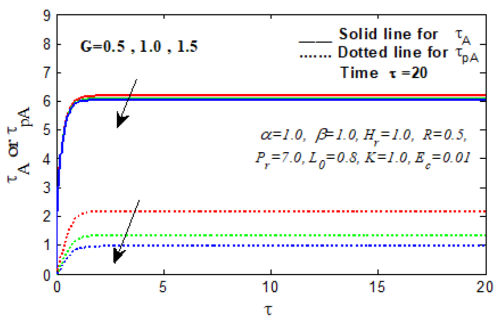

(c) Effect of G on τ_A (orτ_{pA})

Fig. 7.

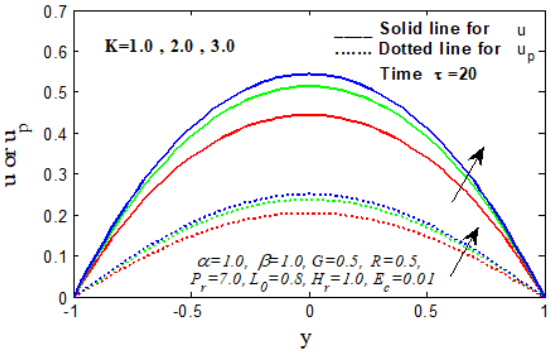

(a) Effect of K on u (oru_p)

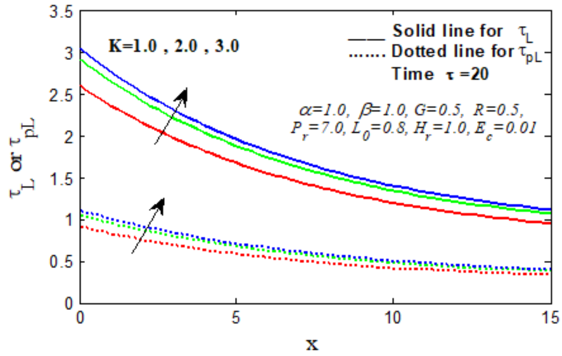

(b) Effect of K on τ_L (orτ_{pL})

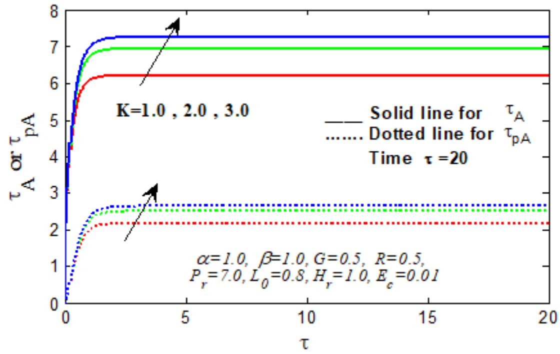

(c) Effect of K on τ_A (orτ_{pA})

Fig. 8.

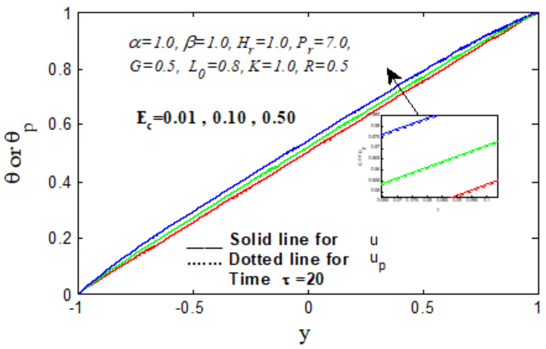

(a) Effect of E_c on θ (orθ_p)

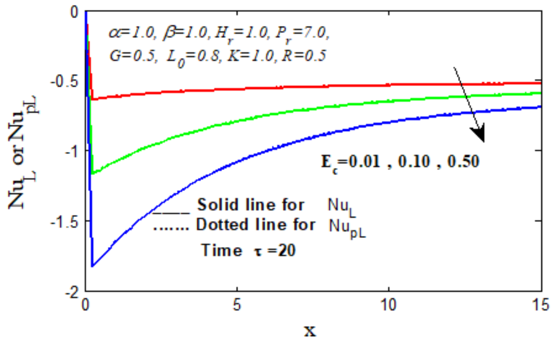

(b) Effect of E_c on Nu_L (orNu_{pL})

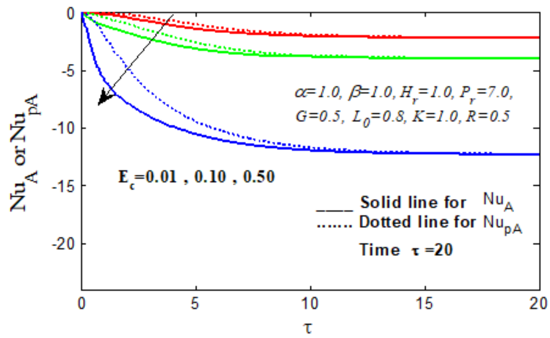

(c) Effect of E_c on Nu_A (orNu_{pA})

Fig. 9.

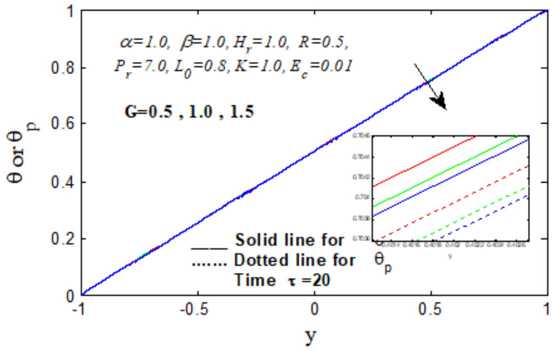

(a) Effect of G on θ (orθ_p)

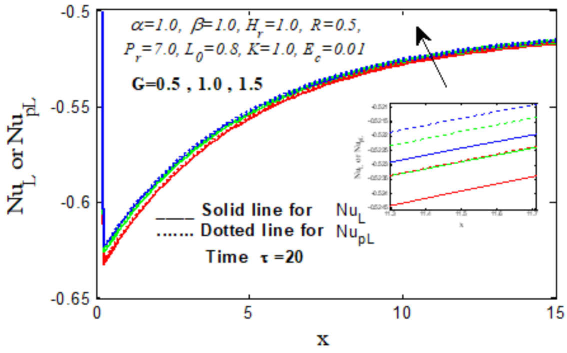

(b) Effect of G on Nu_L (orNu_{pL})

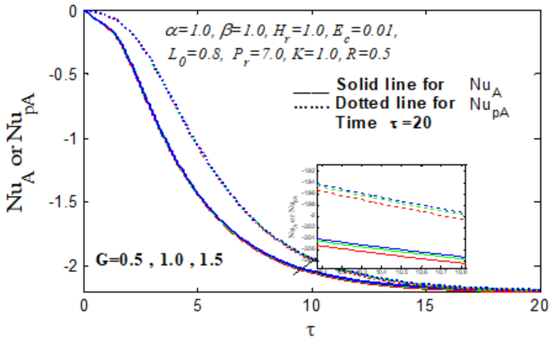

(c) Effect of G on Nu_A (orNu_{pA})

Fig. 10.

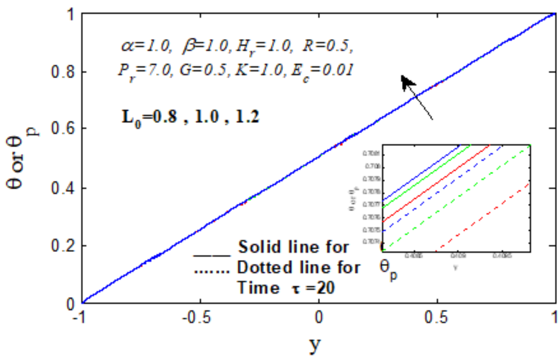

(a) Effect of L_0 on θ (orθ_p)

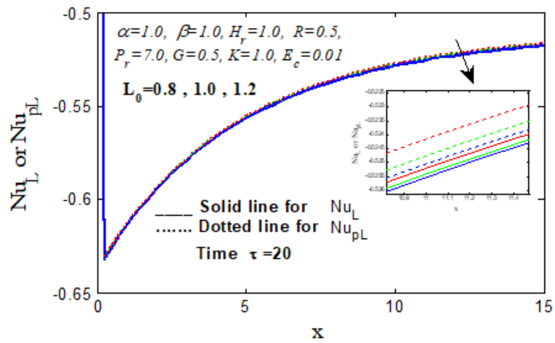

(b) Effect of L_0c on Nu_L (orNu_{pL})

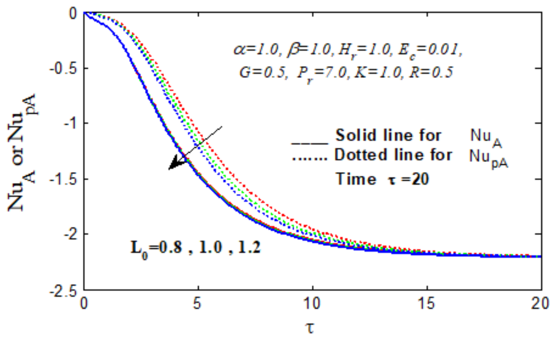

(c) Effect of L_0 on Nu_A (orNu_{pA})

Fig. 11.

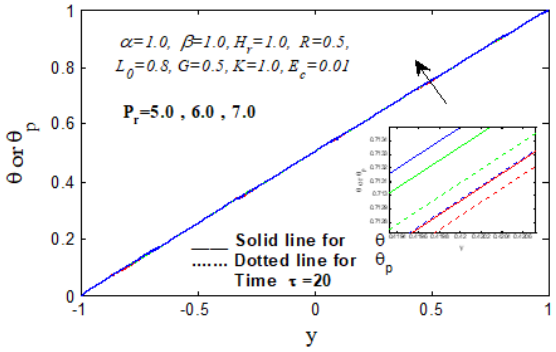

(a) Effect of P_r on θ (orθ_p)

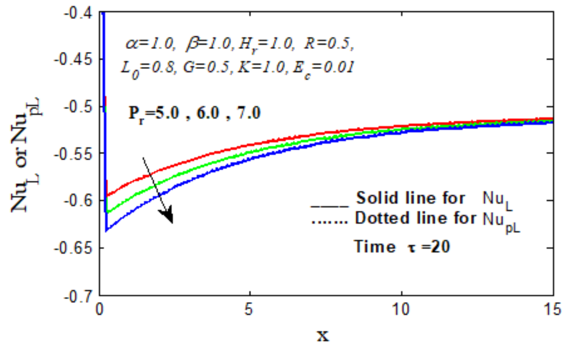

(b) Effect of P_r on Nu_L (orNu_{pL})

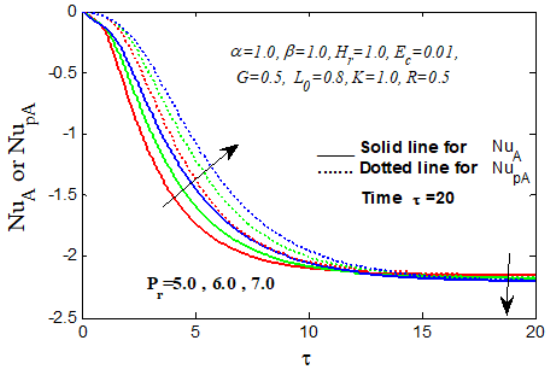

(c) Effect of P_r on Nu_A (orNu_{pA})

Fig. 12.

References

[1] A Gailitis. and O.Leilausis, On a possibility to reduce the hydro dynamical resistance of a plate in an electrode.Appl. Magnetohydrodyn, Vol.12, pp. 143-146, 1961.

[2] A. Pantokratoras, E. Magyari , MHD free-convection boundary layer flow from a riga plate. J.Eng. Maths, Vol.64(3), pp. 303-315, 2009.

[3] L.Wahidunnisa, K.Subbarayudu, S.Suneetha, Effect of viscous dissipation over a Riga plate in a nano fluid with heat source/sink. IJTIMES, Vol.4, Issue.6, 2016.

[4] A. Anjum, N.A. Mir, M. Farooq, M. I. Khan and T. Hayat, Influence of thermal stratification and slip conditions on stagnation point flow towards variable thicked Riga plate. Results in Physics. Vol.9,pp.1021-1030, 2018.

[5] A. Ahmad, Flow Control of Non-Newtonain Fluid using Riga Plate:Reiner-Phillipoff and Powell-Eyring Viscosity Models. Journal of Applied Fluid Mechanics, Vol. 12, No. 1, pp. 127-133, 2019.

[6] T. Hayat, Tehseen Abbas, M. Ayub, M. Faroq, A. Alsaedi, Flow of nanofluid due to convectively heated Riga plate with variable thickness. Vol.222,pp.854-862, 2016.

[7] Z. Iqbal, Ehtsham Azhar, Zaffar Mehmood and E.N. Maraj, Melting heat transport of nanofluidic problem over a Riga plate with erratic thickness: Use of Keller Box scheme, Results in Physics, vol.7, pp.3648–3658,2017.

[8] Z. Iqbal, E. Azhar, Z. MEhmood, E.N. Maraj, Unique outcomes of internal heat generation and thermal deposition on the viscous dissipative transport of viscoplastic fluid over a Riga plate. Communications in Theoretical Physics ,Vol.69, pp. 68-76,2018.

[9] Ayub M, Abbas T, Bhatti MM., Inspiration of slip effects on electromagneto hydrodynamics (EMHD) nano fluid flow through a horizontal Riga plate. Eur Phys J Plus 16193, 2016.

[10] Adeel Ahmed, Saleem Asghar and Sumaira Afzal, Flow of nanofluid past a Riga plate. Journal of Magnetisn and Magnetic Materials.Vol.420, pp. 44-48, 2016.

[11] Ghulam Rasool, Ting Zhang, Anum Shafiq , Hulya Durur, Influence Of Chemical Reaction on Marangoni Convective Flow of Nanoliquid in the Presence of Lorentz Forces and Thermal Radiation: A Numerical Investigation. J. Adv. Nanotechnology, Vol-1 Issue 1 pp.32-49 , 2019.

[12] Ghulam Rasool, Anum Shafiq, Iskander Tlili, Marangoni convective nanofluid flow over an electromagnetic actuator in the presence of first-order chemical reaction. Heat Transfer-Asian Res. Vol. 49: pp. 274–288, 2020. https://doi.org/10.1002/htj.21612

[13] Parul Saxena, Manju Agarwal , Unsteady flow of a dusty fluid between two parallel plates bounded above by porous medium. International Journal of Engineering, Science and Technology, Vol. 6, pp. 27-33, 2014.

[14] Hazem Ali Attia, W. Abbas, Amira M. D. , Salama, Mostafa , A. M. Abdeen , Transient Couette Flow of a Dusty Fluid between Parallel Porous Plates with the Ion slip Effect and Heat Transfer under Exponential Decaying Pressure Gradient. IJIRSET,Vol. 4, Issue 8, 2015.

[15] Hazem Ali Attia and Karem Mahmoud Ewis , Magnetohydrodynamic flow of continuous dusty particles and non-Newtonian Darcy fluids between parallel plates. Advances in Mechanical Engineering, Vol. 11(6) , pp.1–11,2019.

[16] H.A. Attia, A.L. Aboul-Hassan, M.A.M. Abdeen, A.El-Din Abdin, MHD flow of a dusty fluid between two infinite parallel plates with temperature dependent physical properties under exponentially decaying pressure gradient. Bulgarian Chemical Communications, Vol. 46, pp. 320 – 329,2014.

[17] Rajesh Kumar, Unsteady Flow of a Dusty Conducting Fluid between Parallel Porous Plates through Porous Medium with Temperature Dependent Viscosity. IJETR, ISSN: 2321-0869, 2014.

[18] P. Eguia , J. Zueco, E. Granada , D. Patino , NSM solution for unsteady MHD Couette flow of a dusty conducting fluid with variable viscosity and electric conductivity. Applied Mathematical Modelling Vol.35, 303–316, 2011.

[19] G. C. Hazarika and Santana Hazarika, Effects of Variable Viscosity and Thermal Conductivity on the Flow of Dusty Fluid over a Continuously Moving Plate. International Journal of Computer Applications, pp.0975– 8887, Vol. 122, 2015.

[20] O.D. Makinde , T. Chinyoka , MHD transient flows and heat transfer of dusty fluid in a channel with variable physical properties and Navier slip condition. Computers and Mathematics with Applications,Vol. 60, pp.660–669, 2010.

[21] B. J. Gireesha, G. S. Roopa, Channabasappa Shanthappa Bagewadi, Unsteady Flow and Heat Transfer of a Dusty Fluid through a Rectangular Channel. Mathematical Problems in Engineering , 2010, (1024-123X). DOI: 10.1155/2010/898720.

[22] Rebhi A. Damseh, On Boundary Layer Flow of a Dusty Gas from a Horizontal Circular Cylinder. Brazilian Journal of Chemical Engineering, Vol. 27, No. 04, pp. 653 - 662, 2010.

[23] Mudassar Jalil, Saleem Asghar, and Shagufta Yasmeen , An Exact Solution of MHD Boundary Layer Flow of Dusty Fluid over a Stretching Surface .Mathematical Problems in Engineering ,Article ID 2307469, 2017. https://doi.org/10.1155/2017/2307469.

[24] Sharena Mohamad Isa and Nurul Farahain Mohammad , Boundary Layer Flow of Dusty Fluid on a Stretching

Sheet of Another Quiescent Fluid. J. Phys.: Conf. Ser. 819 012027, 2017.

[25] Ramesh G K and B. J. Gireesha, Flow Over a Stretching Sheet in a Dusty Fluid With Radiation Effect. Journal of Heat Transfer, 135(10):102702, 2013. DOI: 10.1115/1.4024587.

[26] Isah Bala Yabo, Basant Kumar Jha, Jeng-Eng Lin, On a Couette Flow of Conducting Fluid. International Journal of Theoretical and Applied Mathematics, Vol.4(1), pp. 8-21, 2018.

[27] A. Mohamed Ismail, Sini Rahuman, K. Sampath Kumar, A Solution of Unsteady Magnetohydrodynamic flow of dusty fluid between parallel porous plates. International Journal of Pure and Applied Mathematics Vol.119, No. 15, pp.1221-1232, 2018.

[28] Monika Srivastava, Dr. Rajeev Khare, Heat and mass transfer in steady Poiseuille flow of fluid between two plates placed in an inclined magnetic field. IJESRT, Vol. 5(11), 2016.